

南極高地からの  
高解像度テラヘルツ天体観測  
High Angular Resolution  
Terahertz Astronomy from Dome A

Hiroshi Matsuo (ATC/NAOJ)

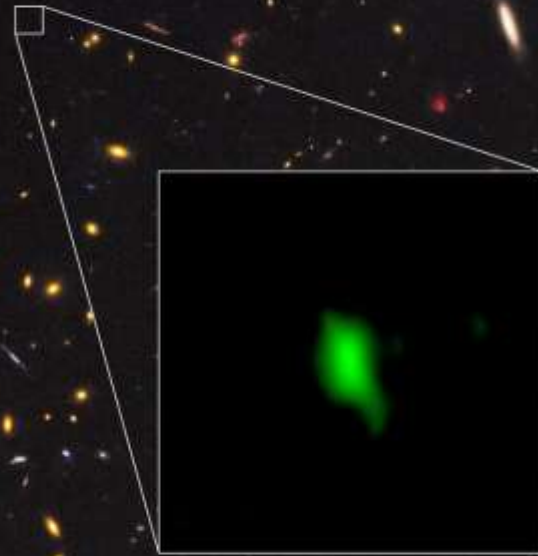
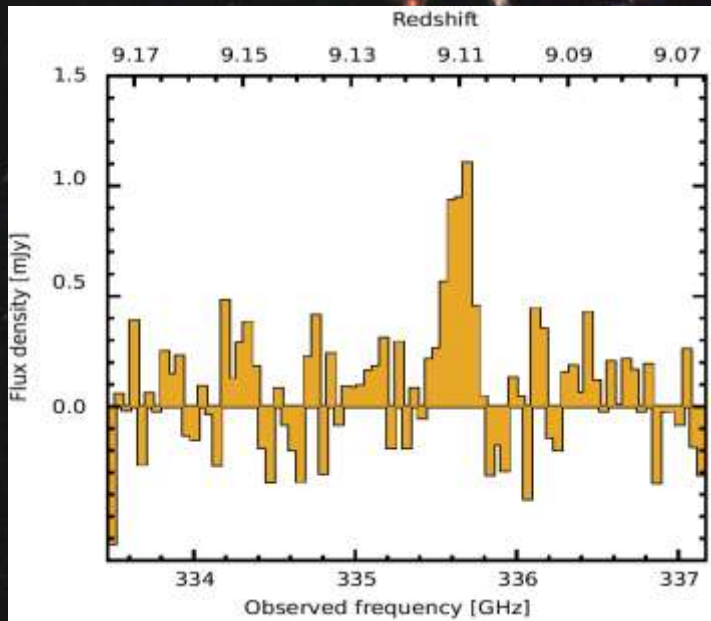
THz Observation

High Angular Resolution

THz Atmosphere

Intensity Interferometry

# The Most Distant $z=9.11$ Spectroscopic Identification with [OIII] $88 \mu\text{m}$

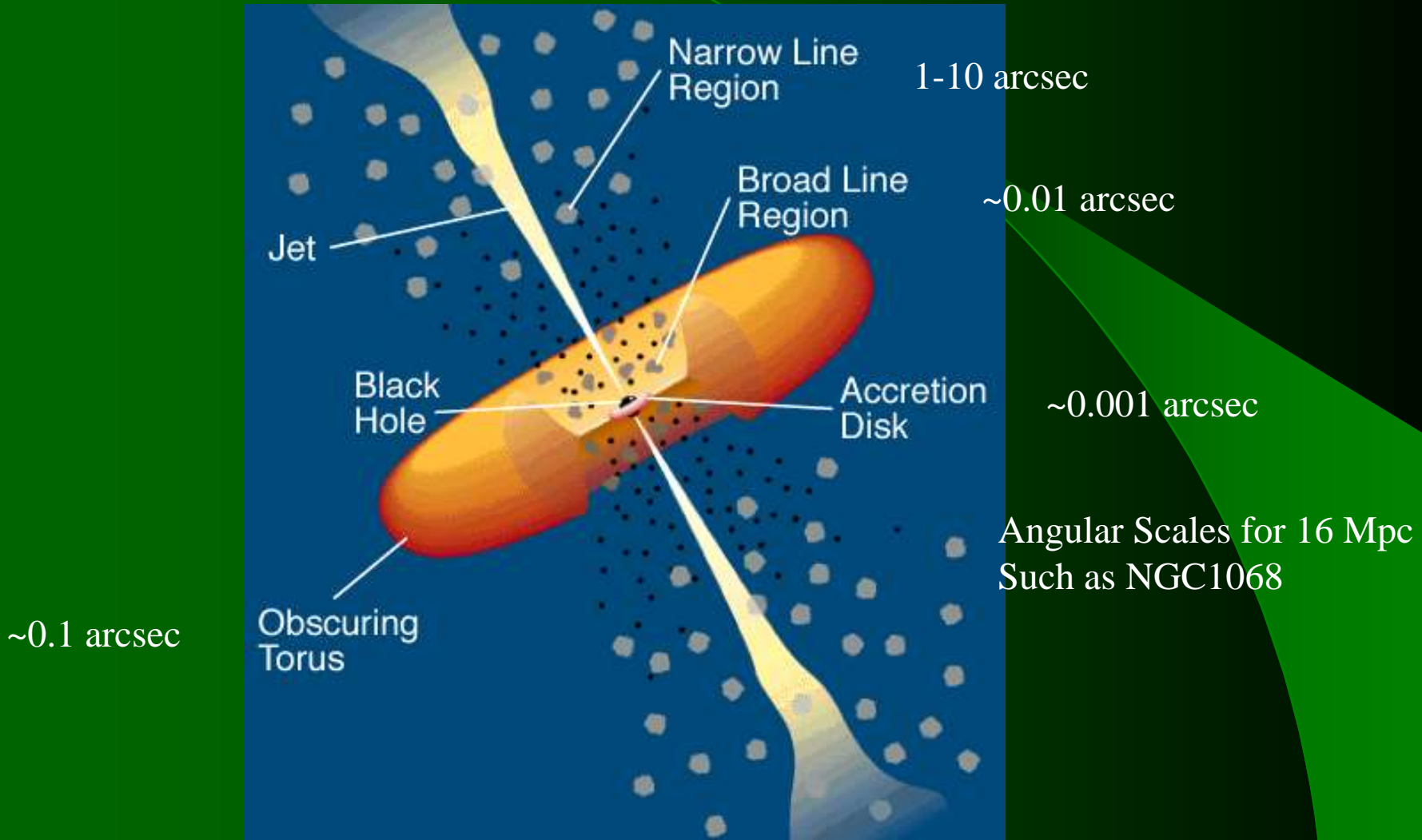


Hashimoto et al., Nature (2018)



Credit: EHT Collaboration

# Structure of an AGN



Urry and Padovani (1995)

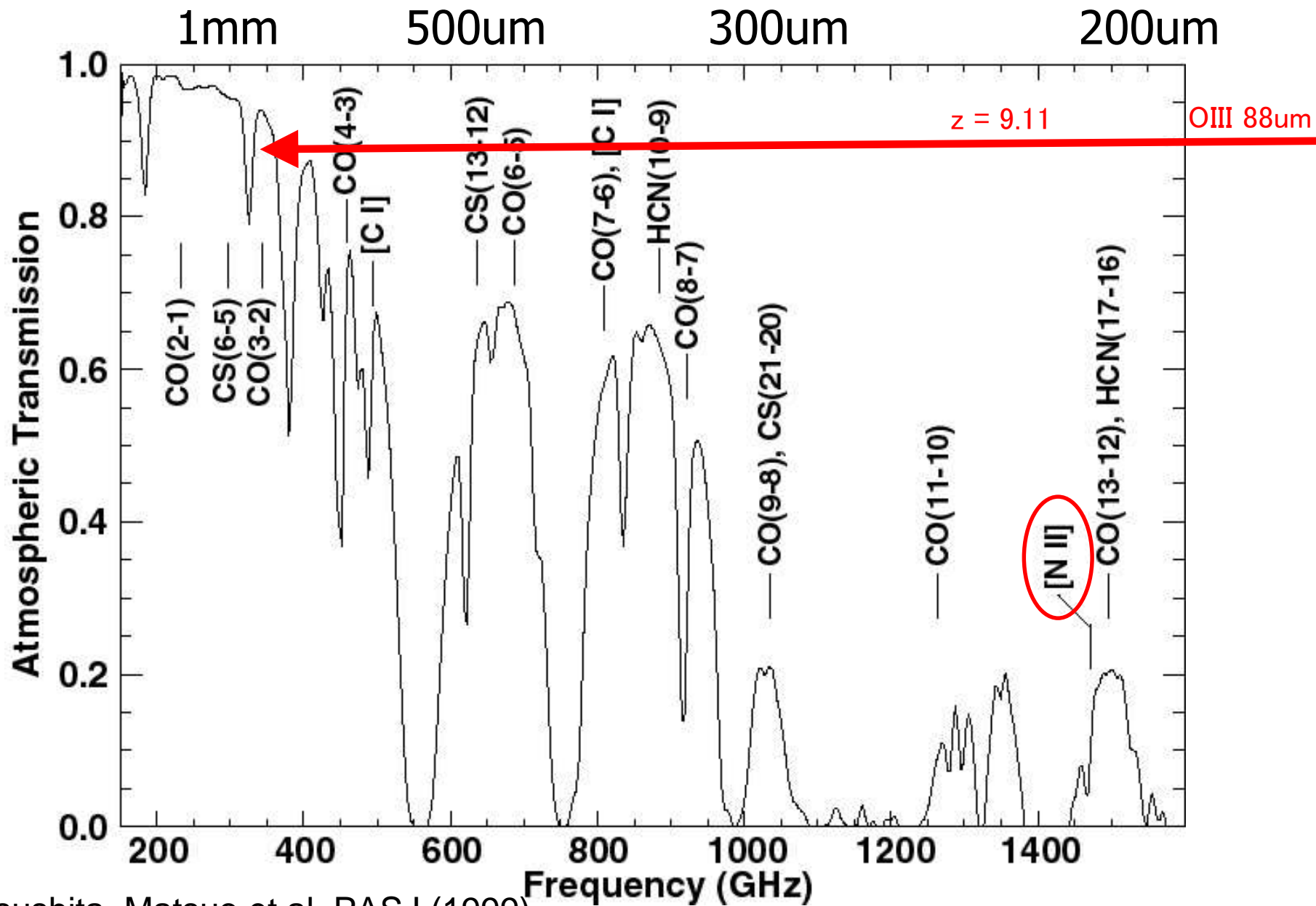
# FIR atomic fine structure lines

		Critical Densities
● OI		
– 63.185 $\mu\text{m}$	4.745THz	$5.0 \times 10^5 \text{ cm}^{-3}$
– 145.54 $\mu\text{m}$	2.060THz	$1.5 \times 10^5 \text{ cm}^{-3}$
● OIII 35.1eV		
– 51.815 $\mu\text{m}$	5.786THz	$3.4 \times 10^3 \text{ cm}^{-3}$
– 88.356 $\mu\text{m}$	3.393THz	$5.0 \times 10^2 \text{ cm}^{-3}$
● NII 14.5eV		
– 121.80 $\mu\text{m}$	2.461THz	$2.8 \times 10^2 \text{ cm}^{-3}$
– 205.30 $\mu\text{m}$	1.460THz	$4.5 \times 10^1 \text{ cm}^{-3}$
● NIII 29.6eV		
– 57.330 $\mu\text{m}$	5.229THz	$3 \times 10^3 \text{ cm}^{-3}$
● CII 11.3eV		
– 157.68 $\mu\text{m}$	1.901THz	$2.7 \times 10^3 \text{ cm}^{-3}$

# FIR atomic fine structure lines

		Critical Densities
● OI		
– 63.185 $\mu\text{m}$	4.745THz	$5.0 \times 10^5 \text{ cm}^{-3}$
– 145.54 $\mu\text{m}$	2.060THz	$1.5 \times 10^5 \text{ cm}^{-3}$
● OIII 35.1eV		
– 51.815 $\mu\text{m}$	5.786THz	$3.4 \times 10^3 \text{ cm}^{-3}$
– 88.356 $\mu\text{m}$	3.393THz	$5.0 \times 10^2 \text{ cm}^{-3}$
● NII 14.5eV		
– 121.80 $\mu\text{m}$	2.461THz	$2.8 \times 10^2 \text{ cm}^{-3}$
– 205.30 $\mu\text{m}$	1.460THz	$4.5 \times 10^1 \text{ cm}^{-3}$
● NIII 29.6eV		
– 57.330 $\mu\text{m}$	5.229THz	$3 \times 10^3 \text{ cm}^{-3}$
● CII 11.3eV		
– 157.68 $\mu\text{m}$	1.901THz	$2.7 \times 10^3 \text{ cm}^{-3}$

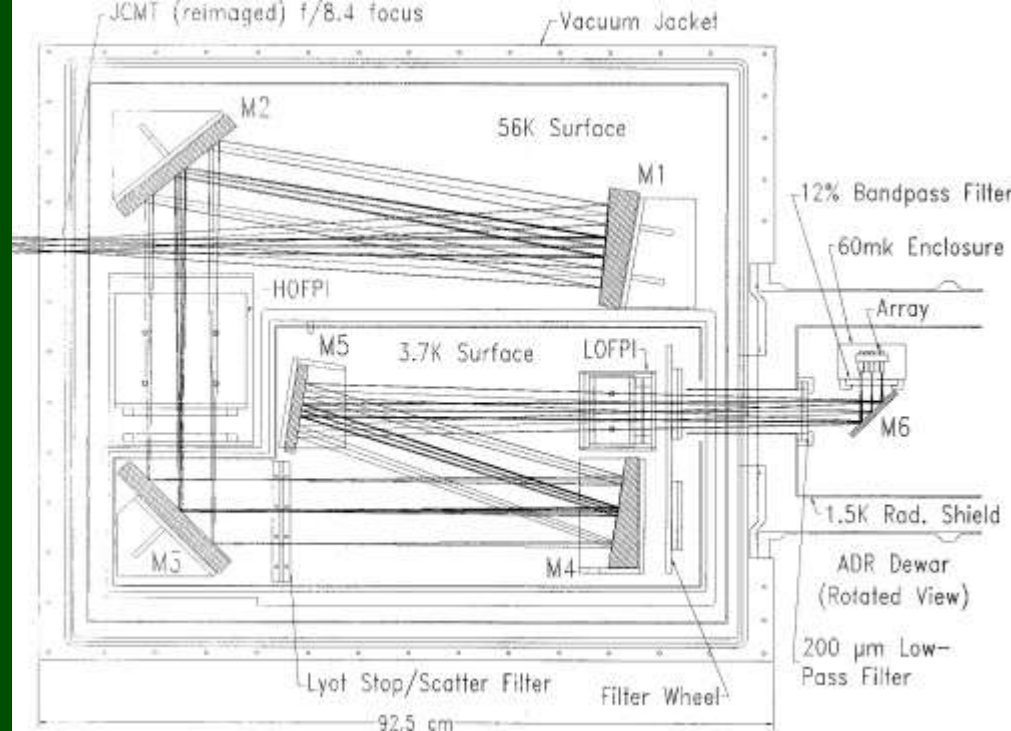
# Atmospheric Windows from Atacama (alt. 4800m)





# AST/RO

# SPIFI



Fabry-Perot  
Spectrometer

5x5 bolometer  
array



From the submillimeter astronomy group, Cornell University

# [NII] 205 $\mu\text{m}$ from South Pole

Atmospheric Transmission  
only 3-6 %

Obserst et al. (2011)

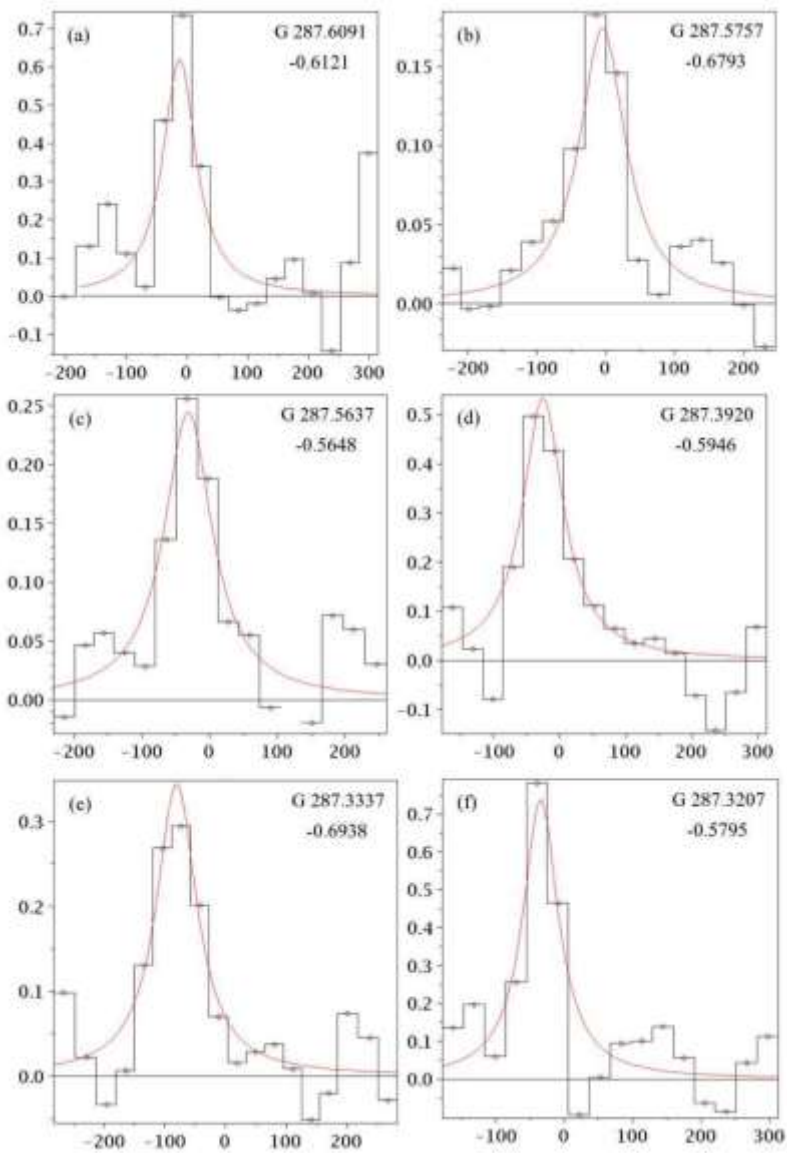
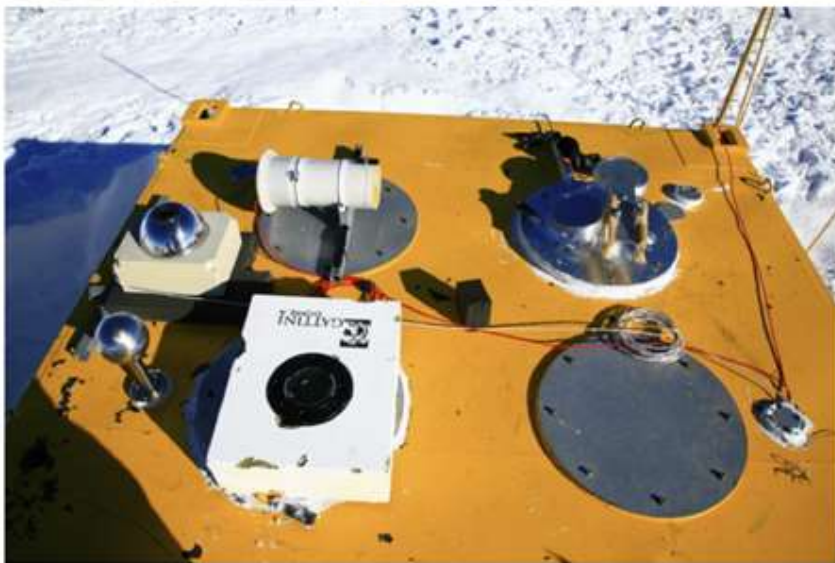
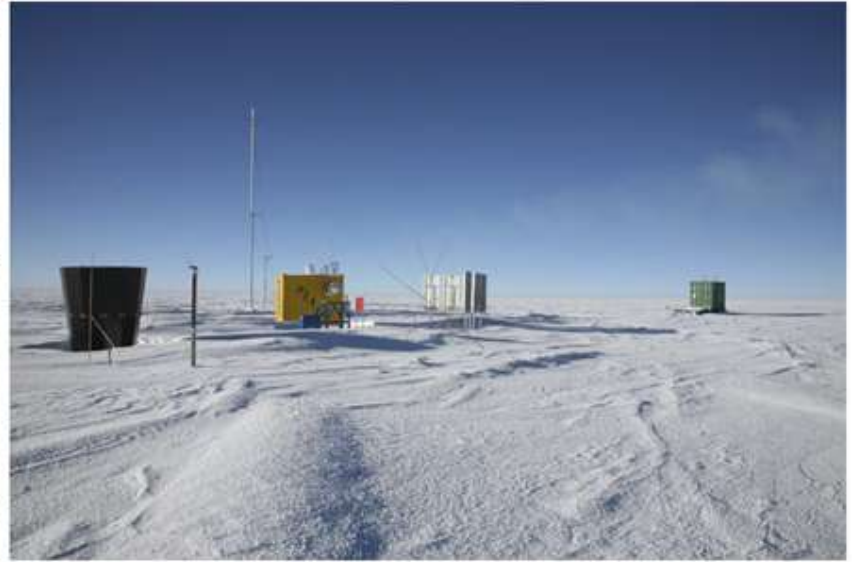


Figure 2.6: Select Detections of the 205  $\mu\text{m}$  [NII] Spectral Line

Spectra in the vicinity of Car II are shown in panels (a), (b), and (c) (SPIFI Car II raster positions 32, 37, and 61, respectively), and spectra in the vicinity of Car I are shown in panels (d), (e), and (f) (SPIFI Car I raster positions 29, 45, and 73, respectively). The  $x$ -axes give the source velocity relative to the Local Standard of Rest (LRS) in units of  $[\text{km s}^{-1}]$ , and the  $y$ -axes give the main beam brightness temperature in units of  $[\text{K}]$ . (The conversion between these units and those of Tables 2.4 and 2.5 is given by Equation 2.8). The (black) data points and bars mark the processed data, and the (red) smooth lines are the least  $\chi^2$  Lorentzian fits. The data have been smoothed with a Hann window.

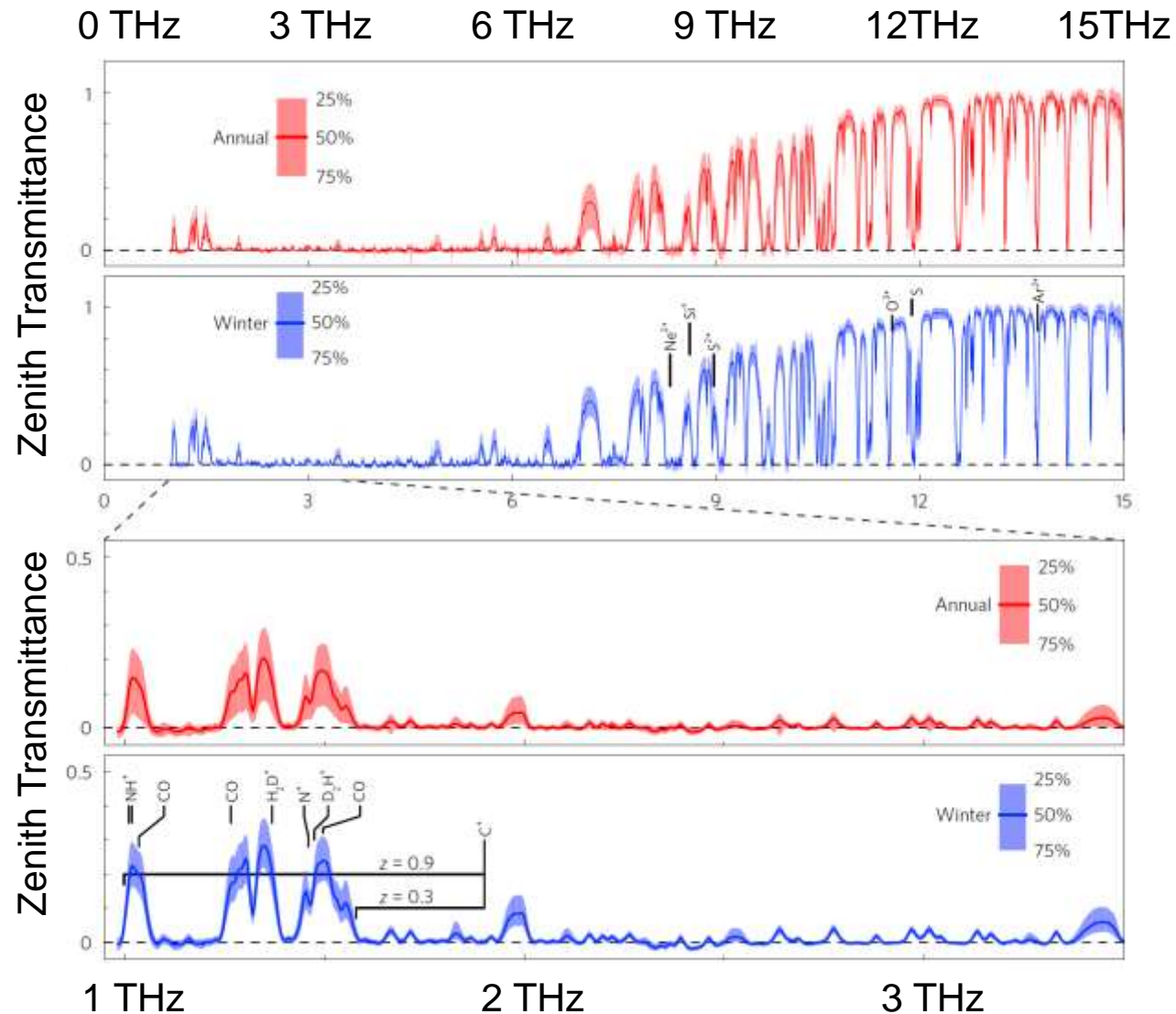
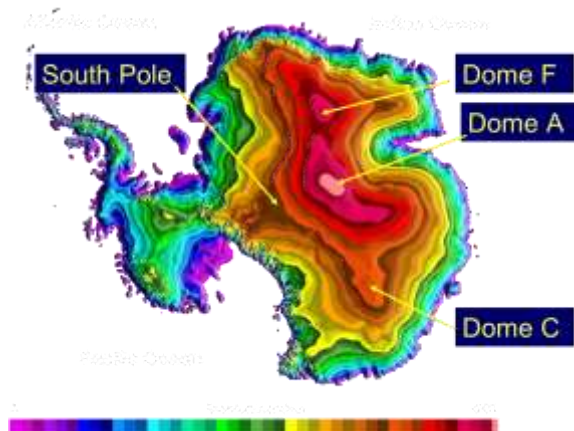
# FTS in Dome A, Antarctica



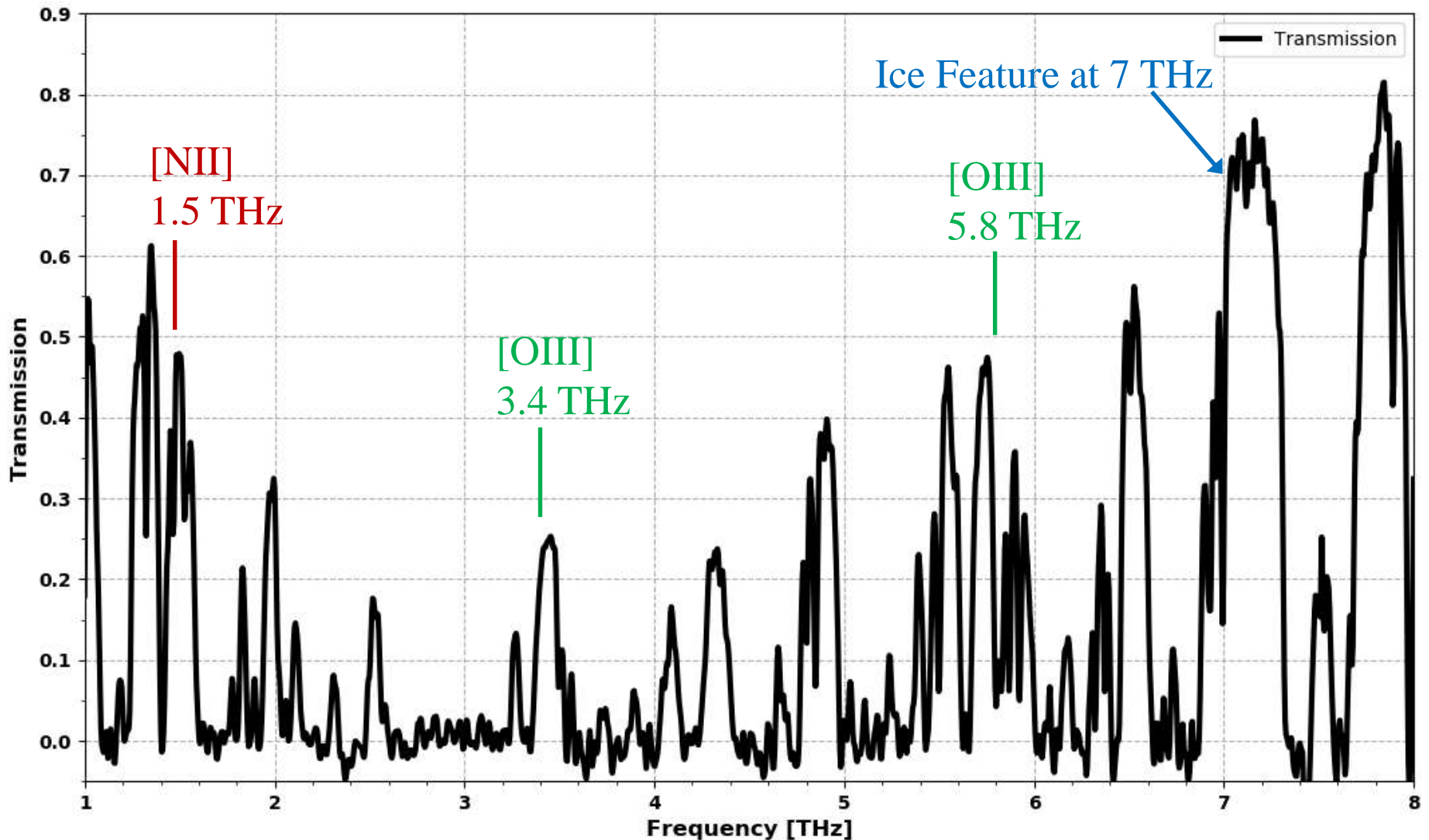
# Terahertz and far-infrared windows opened at Dome A in Antarctica

Annual and winter (April-September) transmittance spectra measured at Dome A during 2010-11.

Shi et al.  
Nature Astronomy (2016)



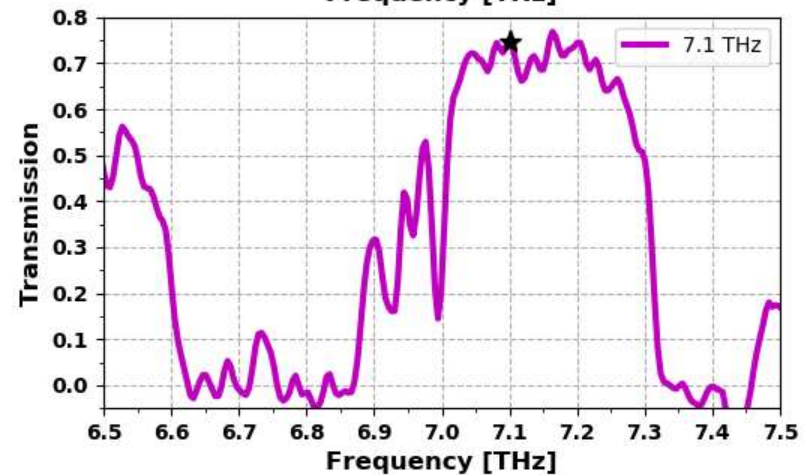
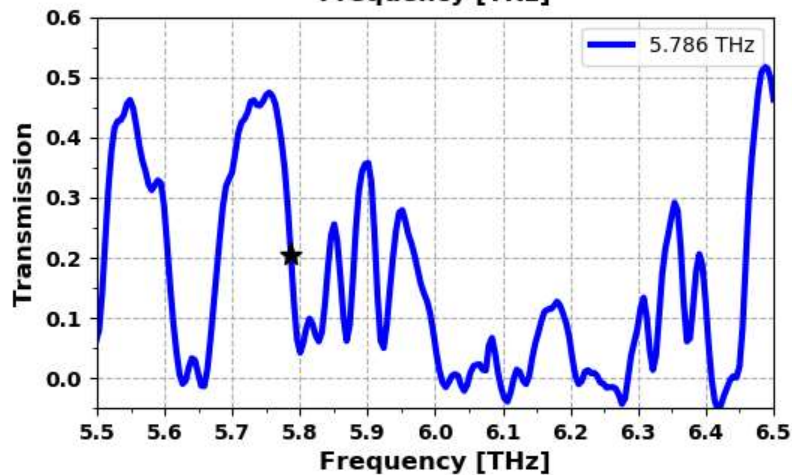
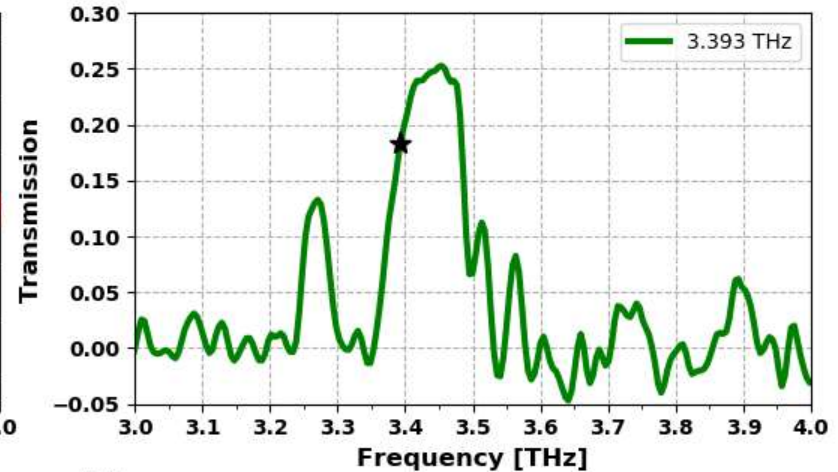
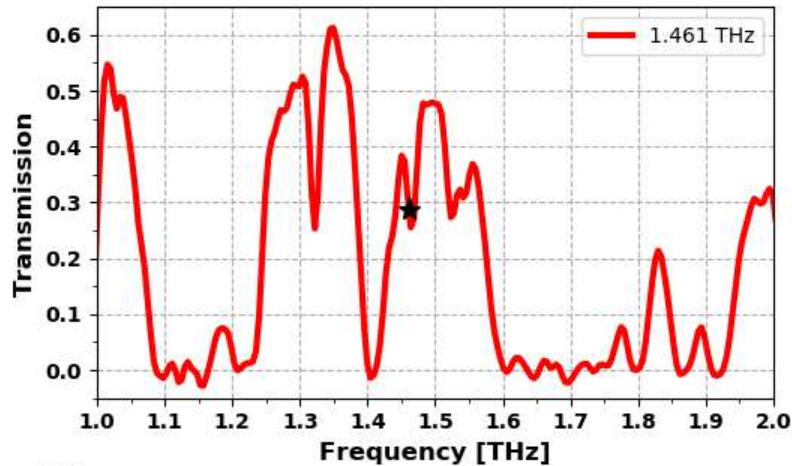
# The Most Transparent Atmosphere



August 9<sup>th</sup> 12–18h UTC, 2010

Matsuo et al. APS (2019)

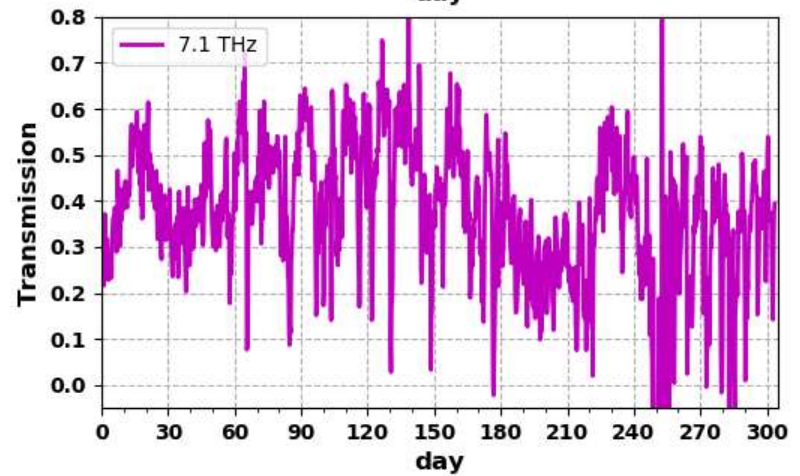
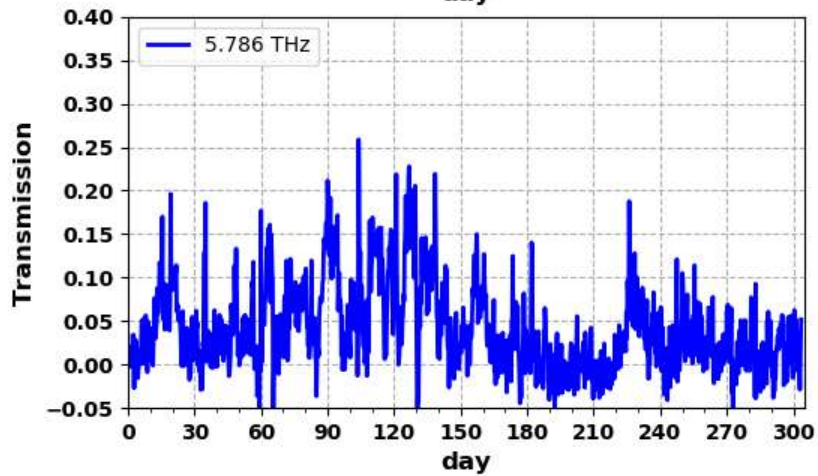
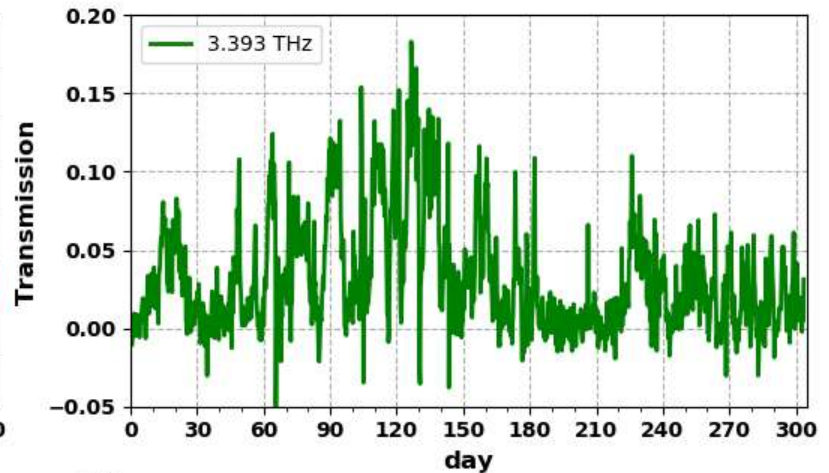
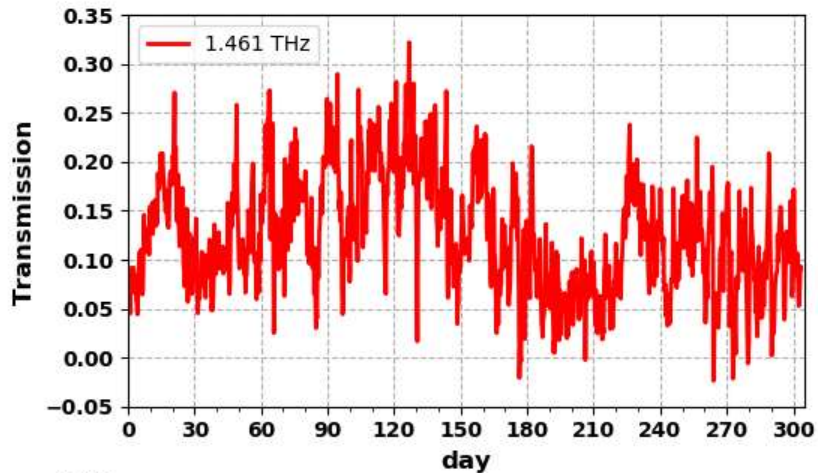
# Windows for [NII], [OIII] and Ice Feature



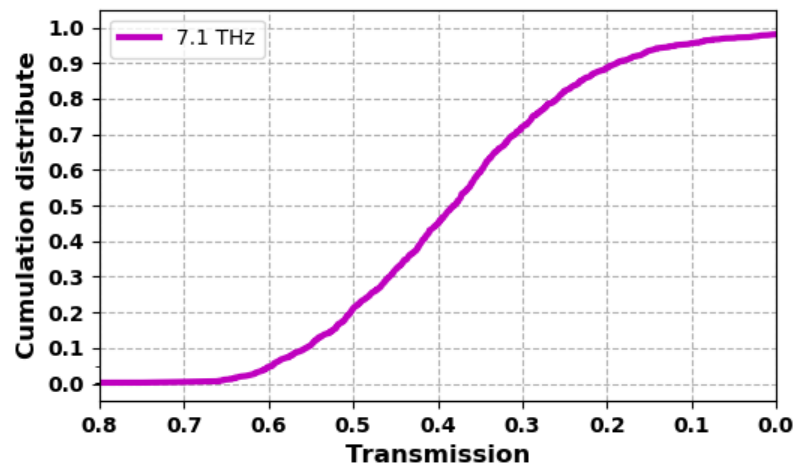
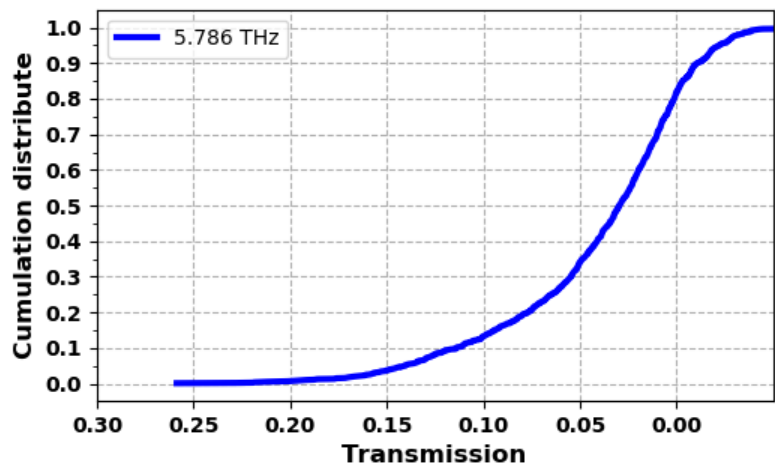
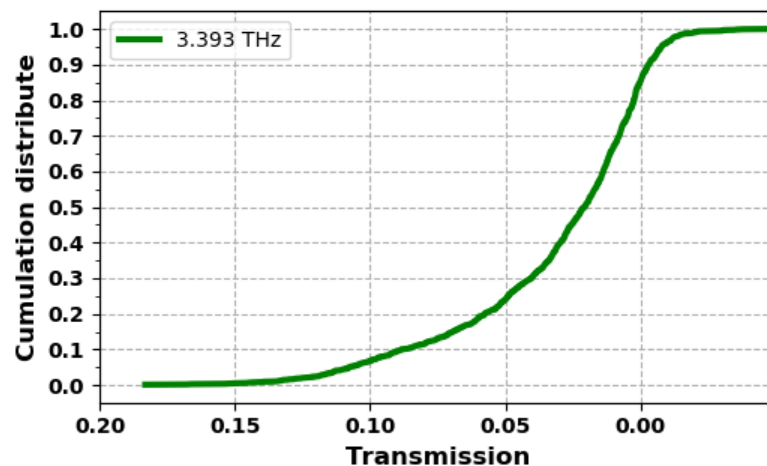
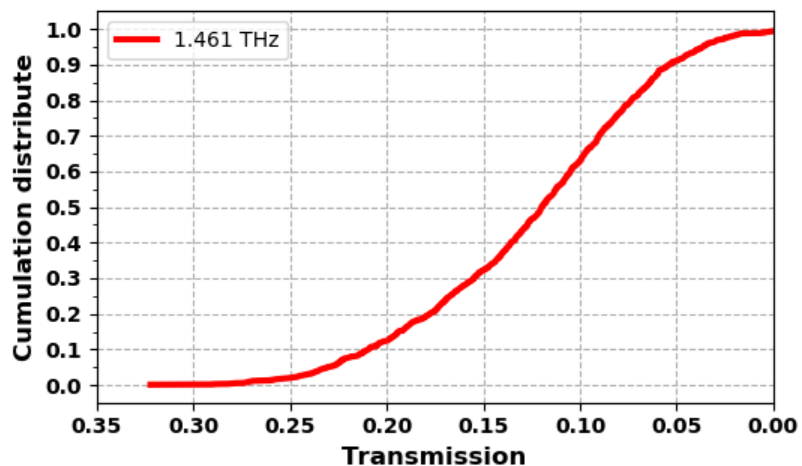
August 9<sup>th</sup> 12–18h UTC, 2010

Matsuo et al. APS in press

# Transmission at 4 windows

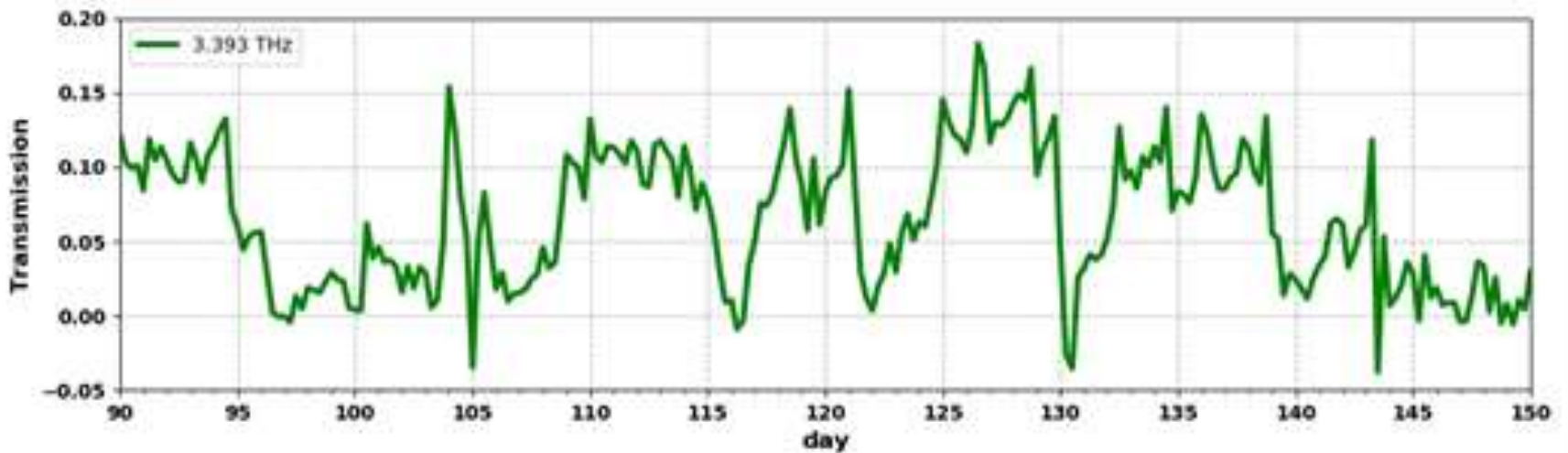


# Cumulative Analysis (Apr.-Sep.)



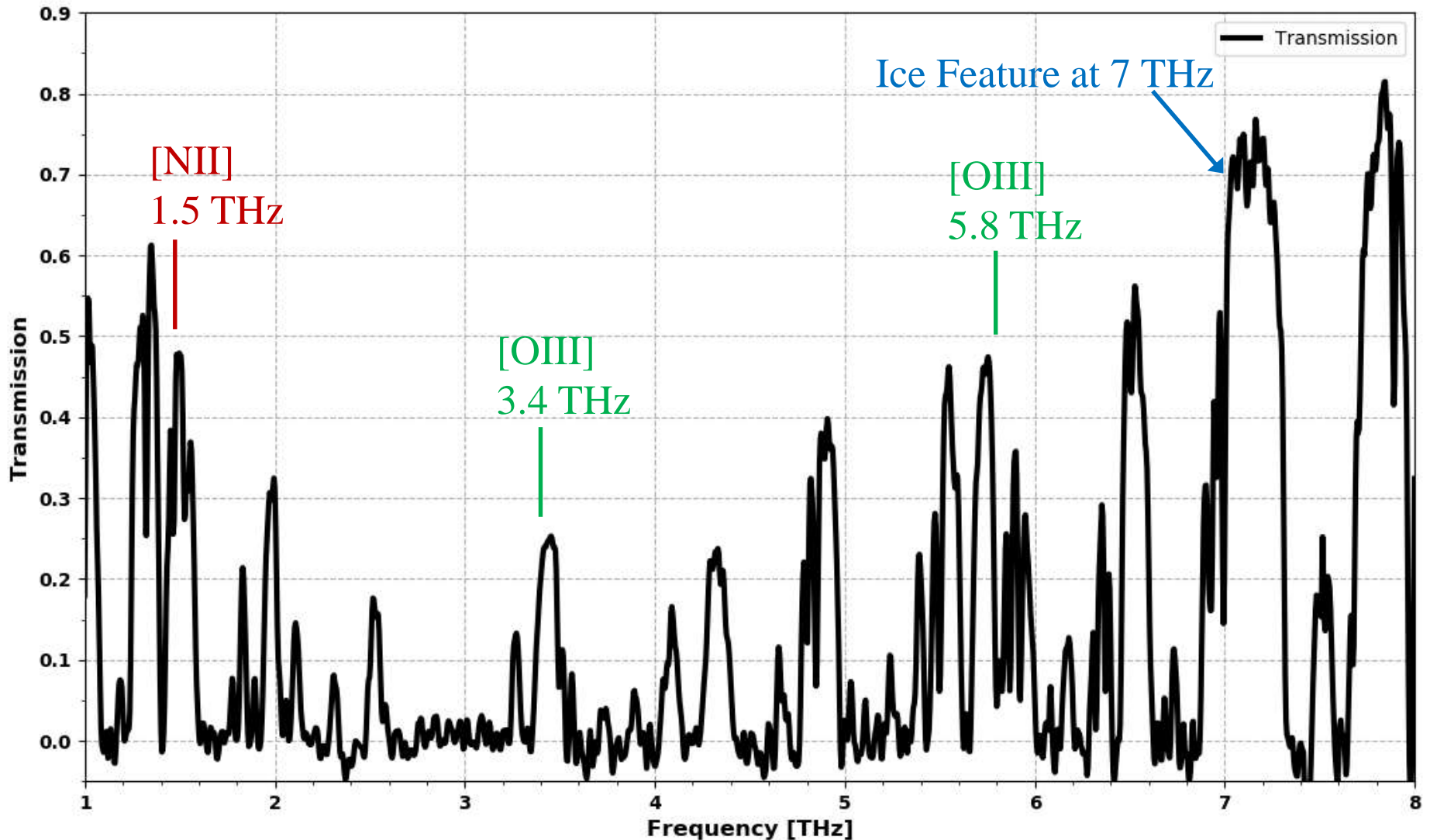


# Can we observe [OIII] 88 $\mu\text{m}$ at 3.393 THz ?



in July - August, 2010

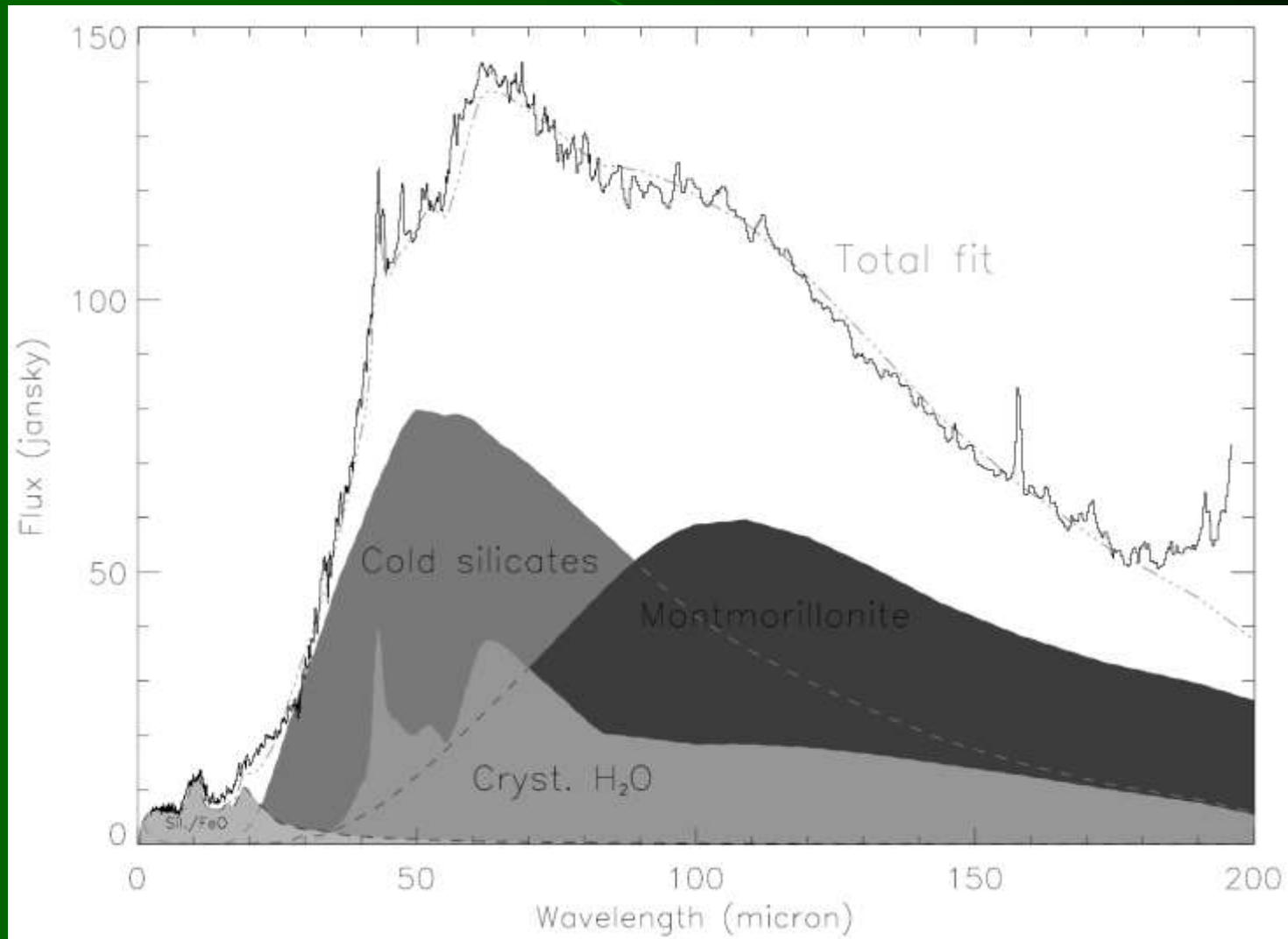
# The Most Transparent Atmosphere



August 9<sup>th</sup> 12–18h UTC, 2010

Matsuo et al. APS (2019)

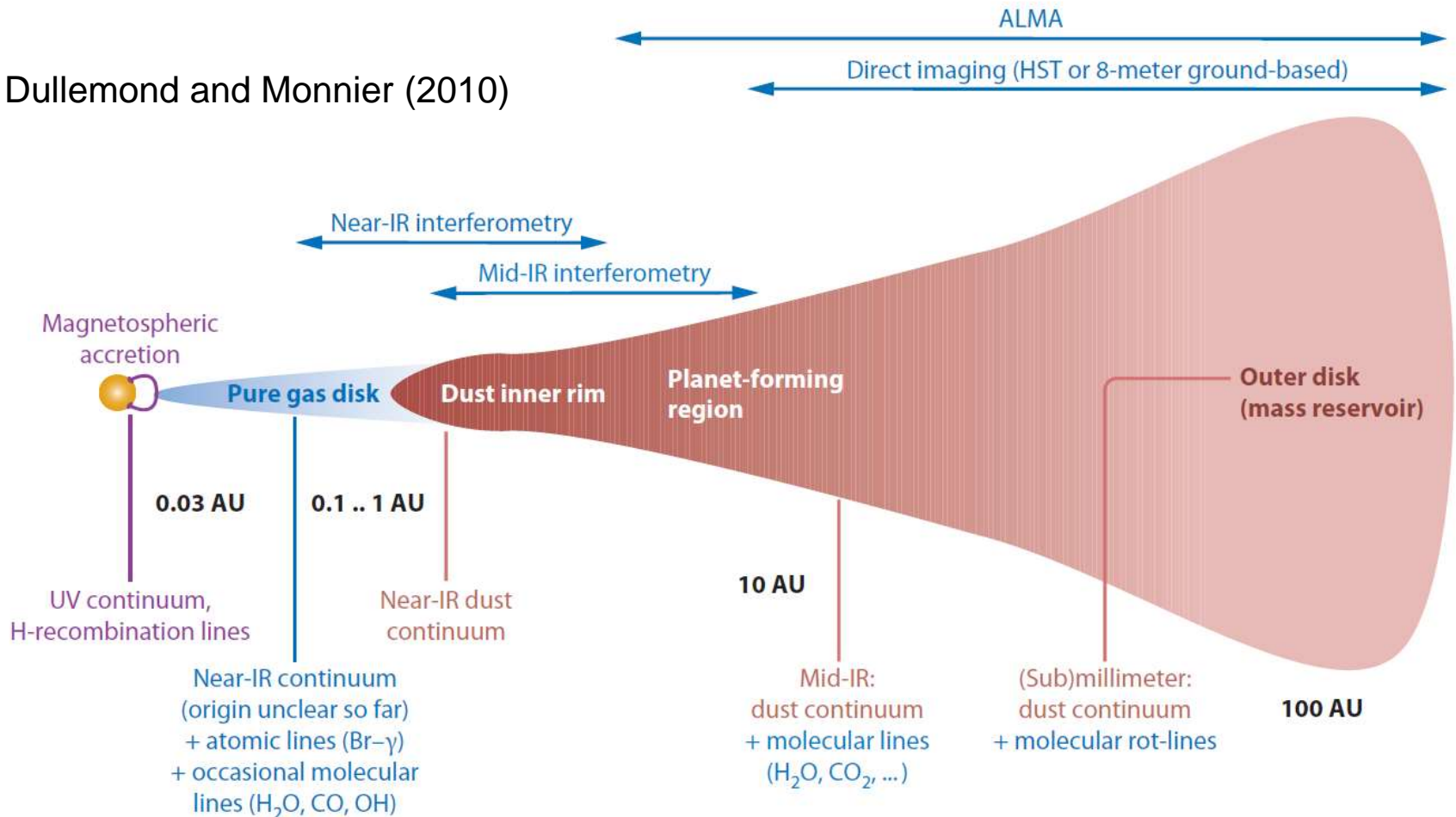
# Water ice feature of HD142527 by ISO



Malfait et al. (1999)

# Structure of a protoplanetary disk

Dullemond and Monnier (2010)

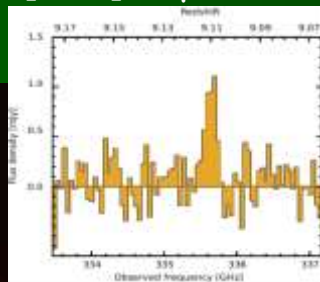


Scales are for Taurus and Auriga region

# Heterodyne or Intensity ?

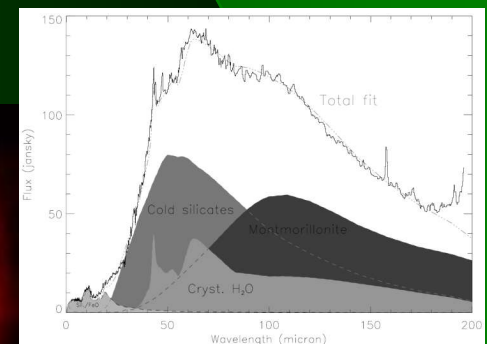
- Start with heterodyne interferometry
  - Shorter baselines, [NII]
- Challenge with intensity interferometry
  - Longer baselines, [OIII] and water ice feature

[OIII] 88 $\mu$ m



Hashimoto et al. (2018)

Water ice feature

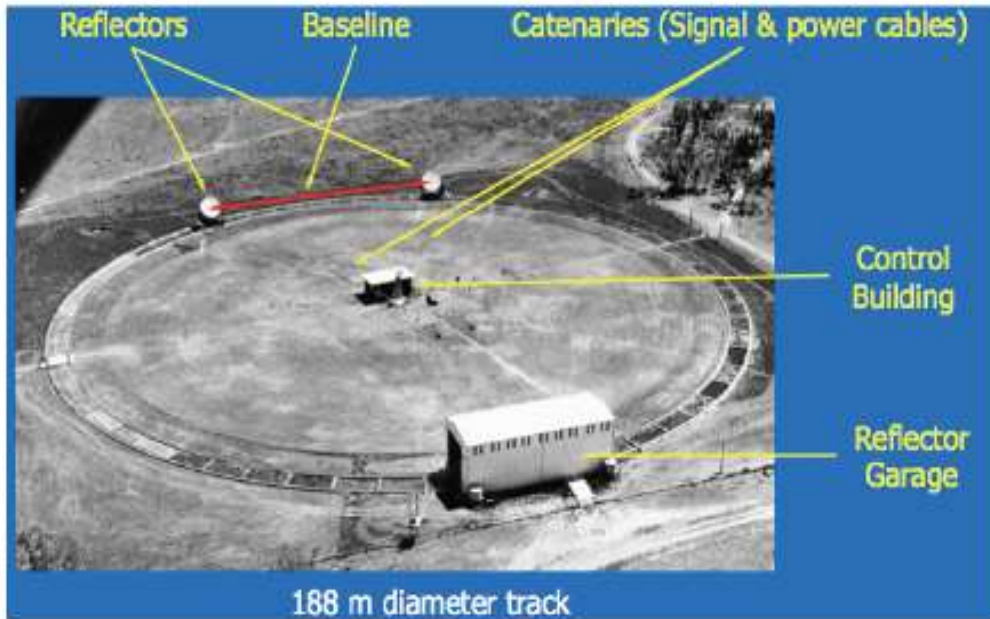


HD142527

Malfait et al. (1999)

ALMA (ESO/NAOJ/NRAO)

# Narrabri Stellar Intensity Interferometer



Narrabri Stellar Interferometer

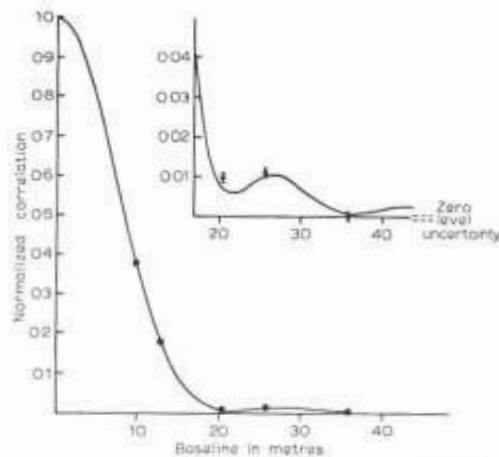
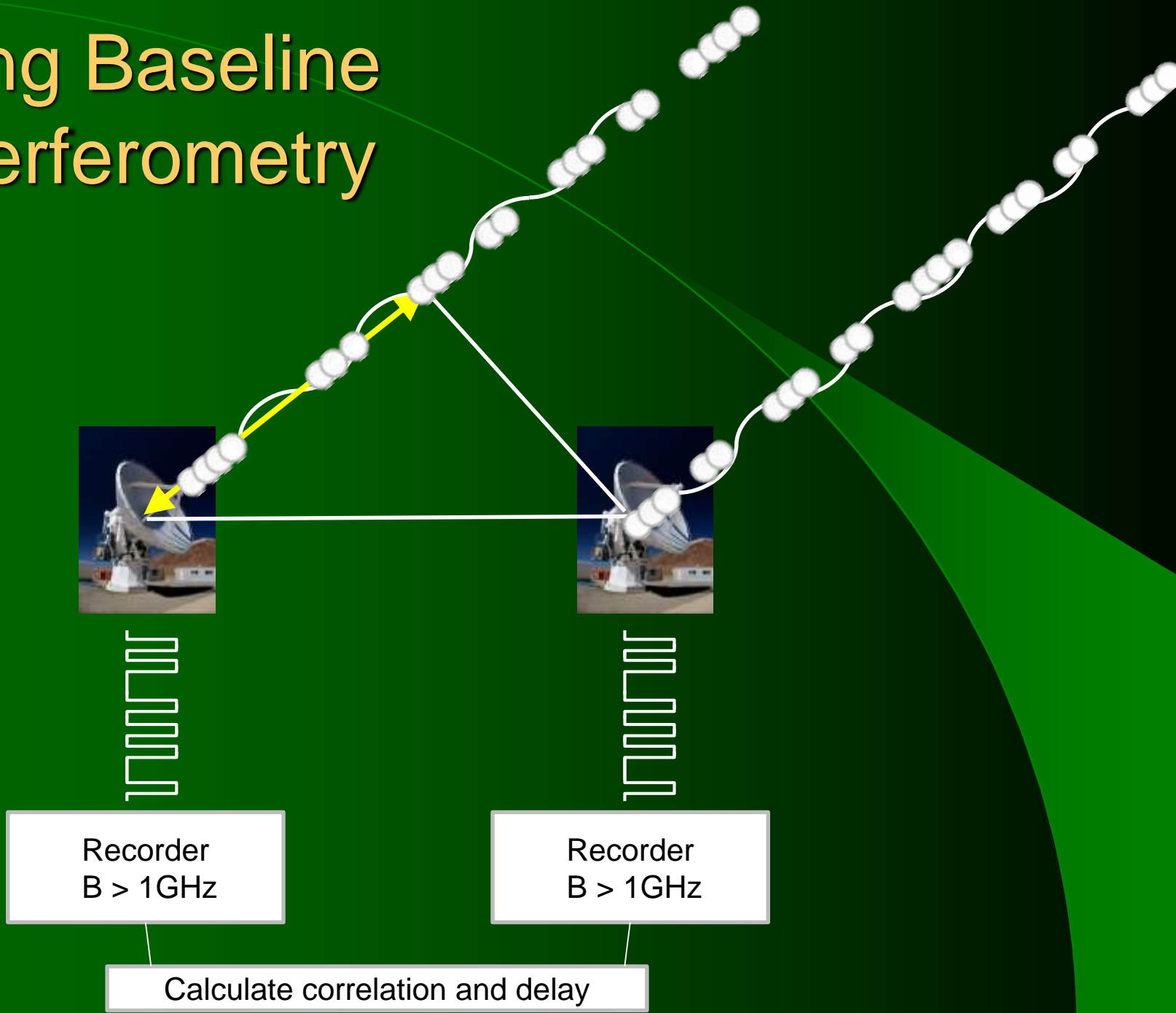


Fig. 11.5. Correlation as a function of baseline for Sirius A ( $\approx$  C Ma). The points show the observed results; the full line shows the theoretical curve for a model atmosphere ( $T_e=10\,000$  K,  $\log g=4$ ,  $\lambda=450$  nm). Results for three long baselines are shown on an expanded scale together with their r.m.s. uncertainties. (Total exposure 203 hours.)

Hanbury-Brown et al. (1974)  
Diameter of 32 early-type stars  
were measured.

# Long Baseline Interferometry

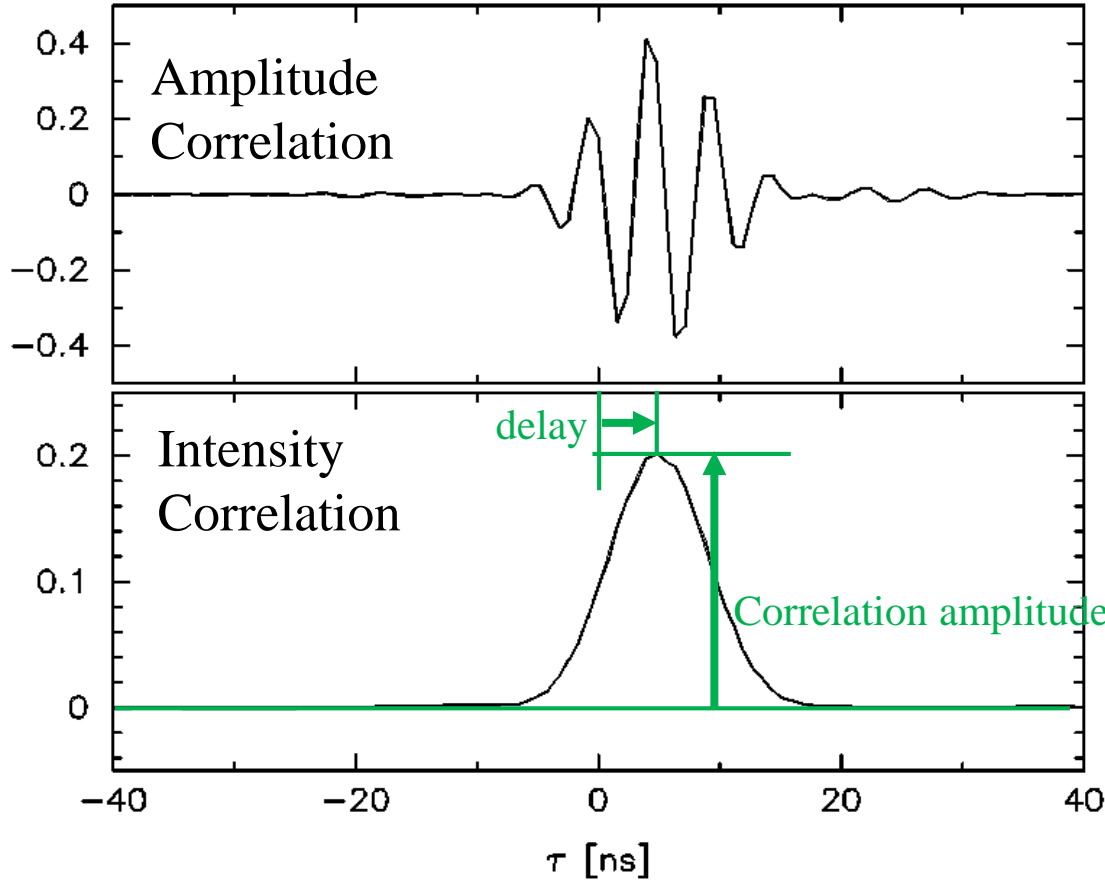


Recorder  
B > 1GHz

Recorder  
B > 1GHz

Calculate correlation and delay

# Nobeyema Radioheliograph at 17 GHz



Antenna Temperature  $T_A^*$  [K]

System Temperature  $T_{\text{sys}}$  [K]

Frequency  $\nu$  [Hz]

Bandwidth  $\Delta\nu$  [Hz]

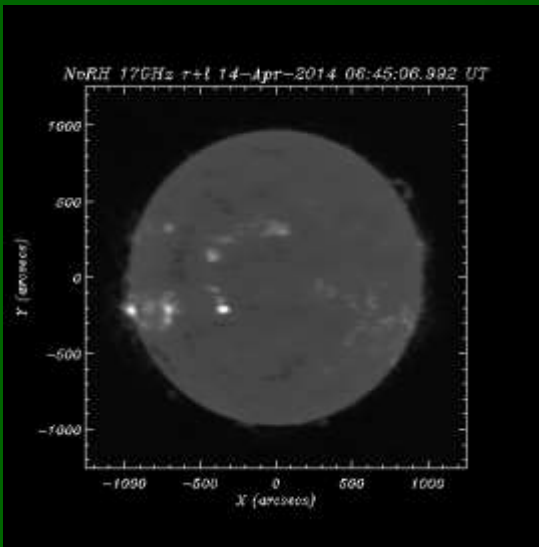
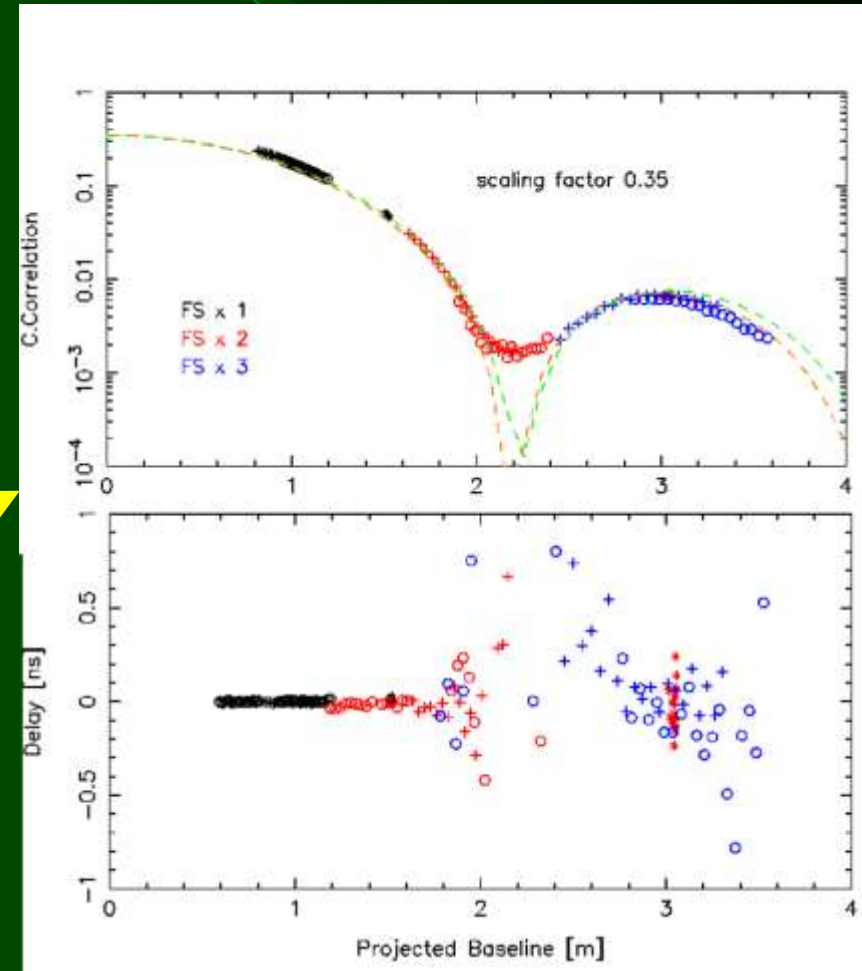
$$\Delta t = \frac{T_{\text{sys}}}{T_A^*} \cdot \frac{1}{\sqrt{\Delta\nu \cdot \tau}} \cdot \frac{1}{\Delta\nu} \text{ [s]}$$

$$\Delta\varphi = 2\pi\nu\Delta t \text{ [rad]}$$



# Experiment at 17 GHz with Nobeyama Radioheliograph

- Real Part
  - (Intensity Correlation)<sup>0.5</sup>
- Imaginary Part
  - $\Delta\phi = 2 \pi \nu \Delta t$



Van Cittert  
Zernike

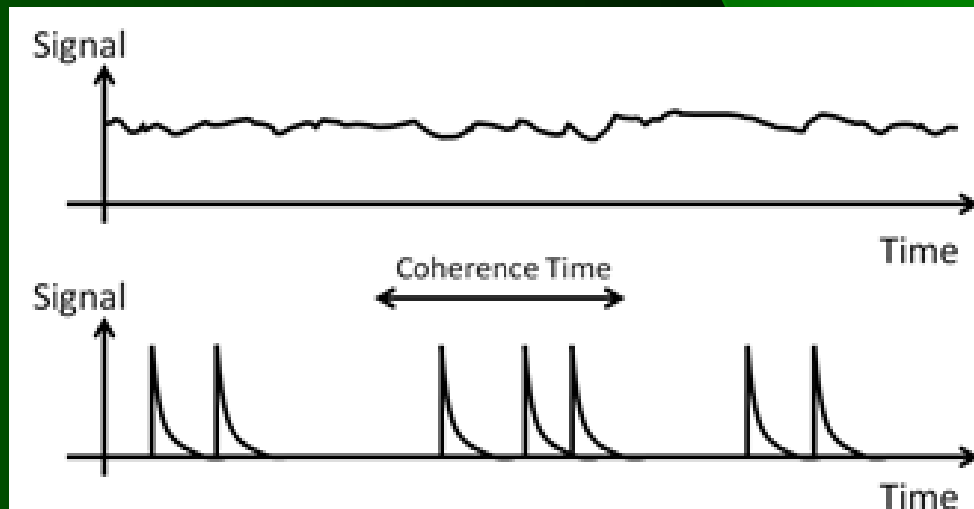


# Requirements to Detectors

- Sensitive to THz photons
  - Photon energy  $\sim 10^{-21}$  Joule
- Fast response
  - 1 GHz bandwidth for 100 M photons/s
- NEP(Noise Equivalent Power)

$$10^{-21} \times (1 \text{ GHz})^{0.5}$$

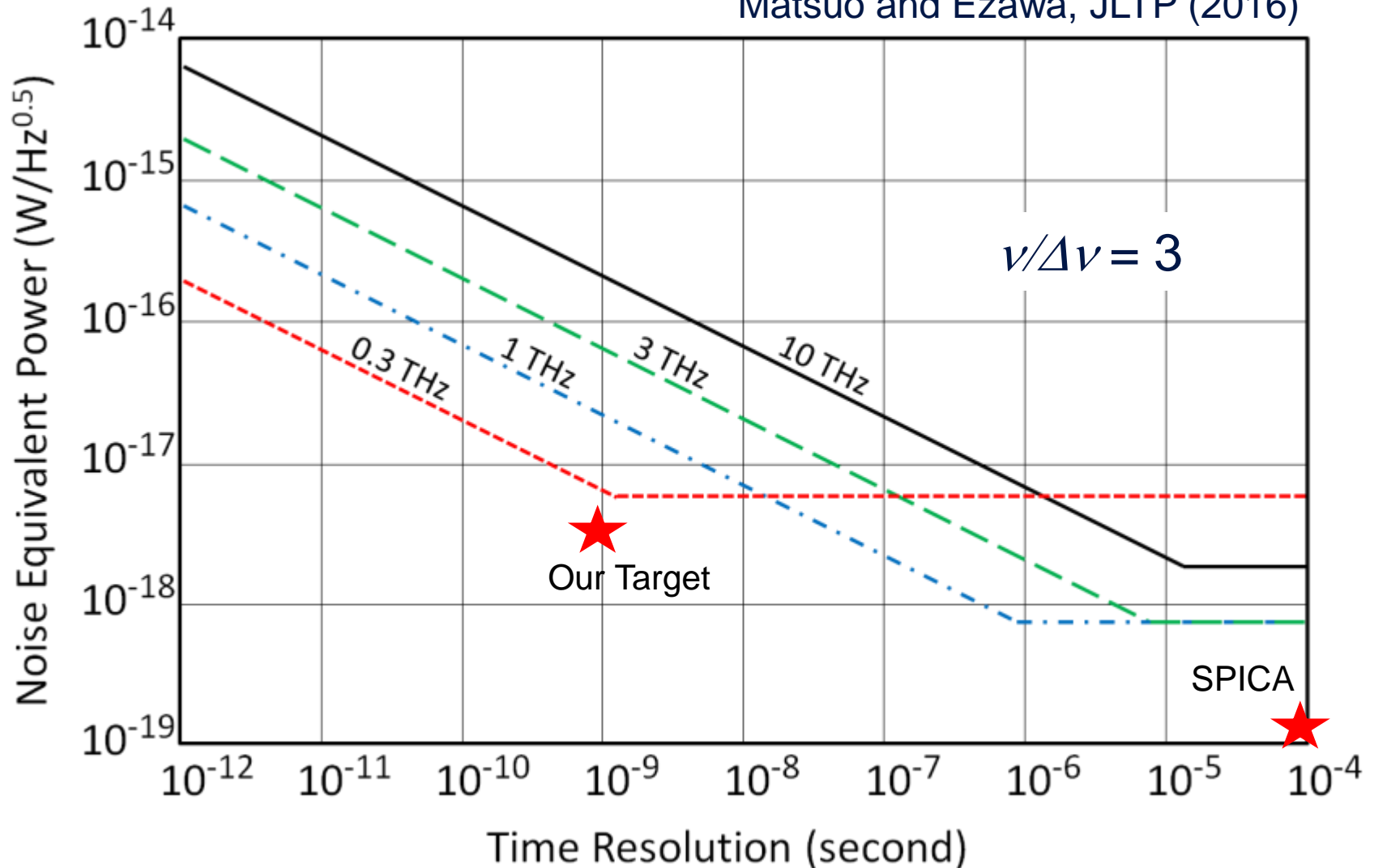
$$\sim 10^{-17} \text{ W/Hz}^{0.5}$$



# NEP for photon counting vs. time resolution

$$\text{NEP} = h\nu/\sqrt{\tau}$$

Matsuo and Ezawa, JLTP (2016)



# SIS Photon Detectors

$$S = \eta \cdot \frac{e}{h\nu} \quad [\text{A/W}]$$

$$N = \sqrt{2eI_0} \quad [\text{A}/\sqrt{\text{Hz}}]$$

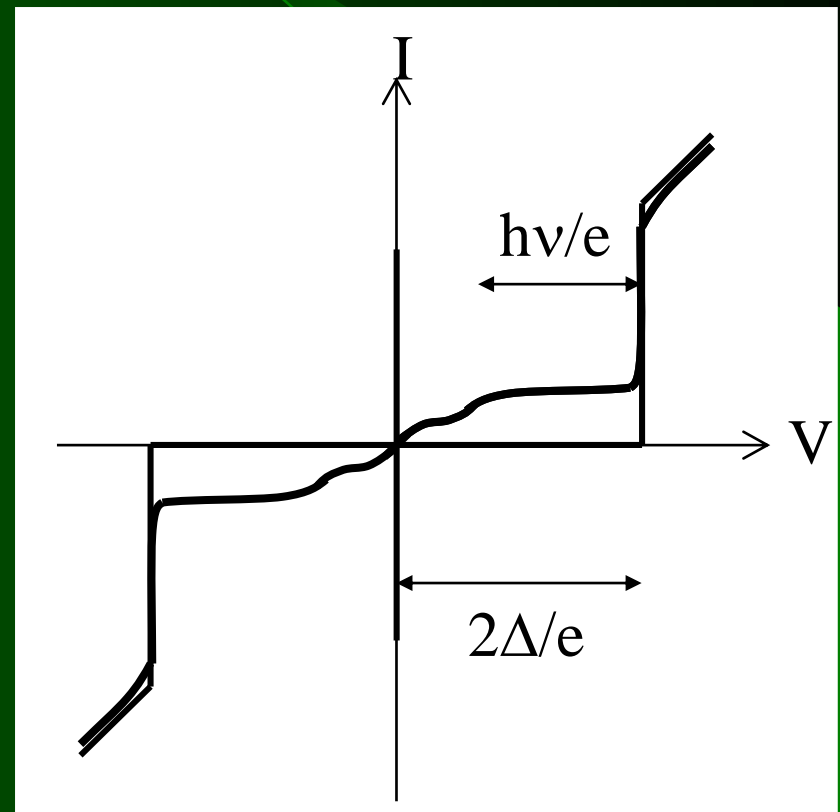
$$NEP = \frac{h\nu}{\eta} \cdot \sqrt{\frac{2I_0}{e}} \quad [\text{W}/\sqrt{\text{Hz}}]$$

$$NEP \approx 3 \times 10^{-18} \text{ W}/\sqrt{\text{Hz}}$$

$$\text{for } I_0 = 1 \text{ pA } \eta = 0.5$$

at 650 GHz

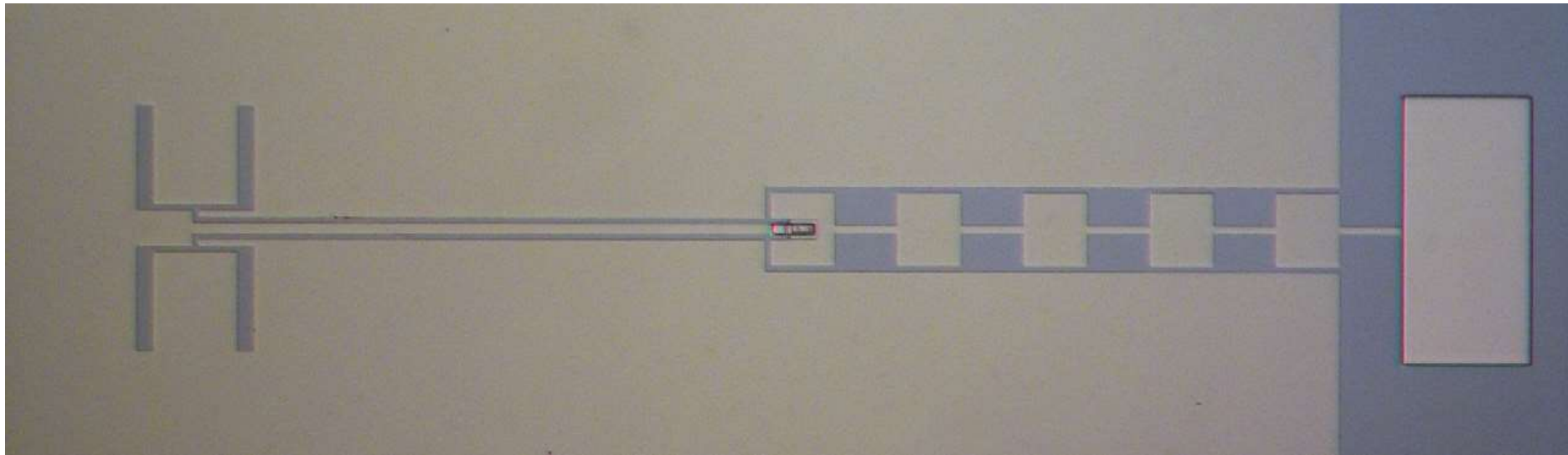
Photon Assisted Tunneling



# Design Parameters

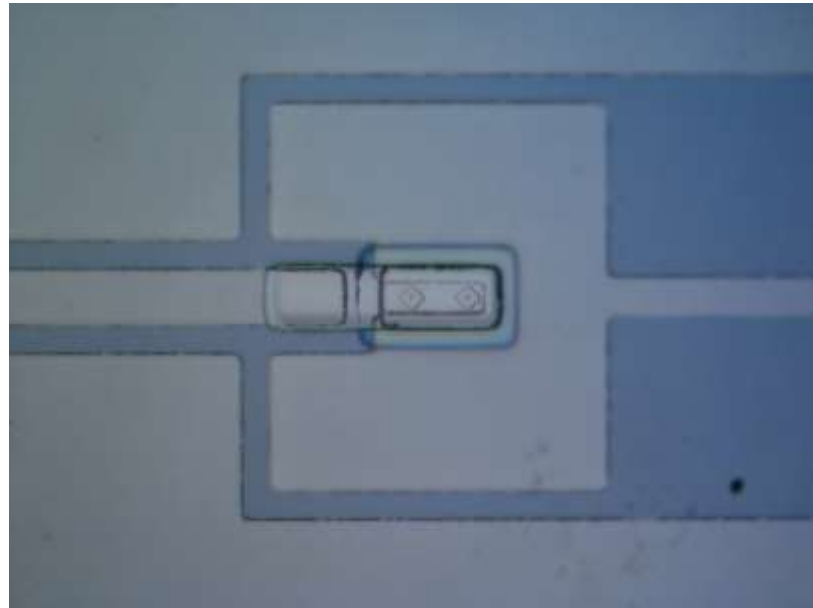
- Nb-SIS  $3 \times 3 \mu\text{m}^2$  with  $J_c = 300 \text{ A/cm}^2$
- $R_n \sim 100 \Omega$ 
  - $\omega R_n C_j \sim 150$  at 500 GHz
  - $\Delta\nu \sim 3 \text{ GHz}$
- Parallel Connected Twin Junction
- Twin-slot antenna and  $50 \Omega$  CPW
- Readout using low gate leakage transistors
  - GaAs-JFETs

# Antenna, CPW, PCTJ, Choke

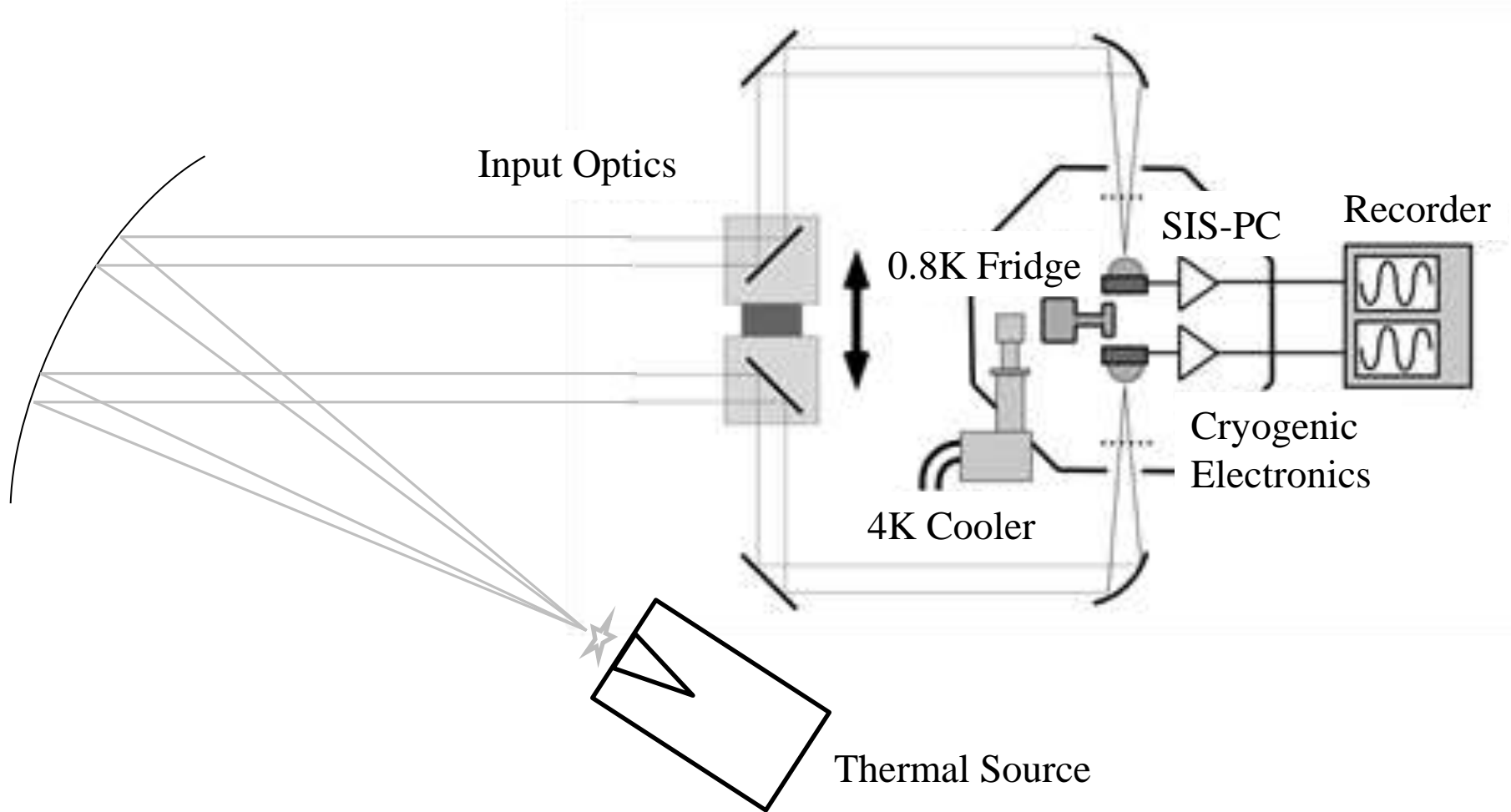


An antenna-coupled Nb-SIS  
photon detector at 500 GHz  
fabricated in CRAVITY

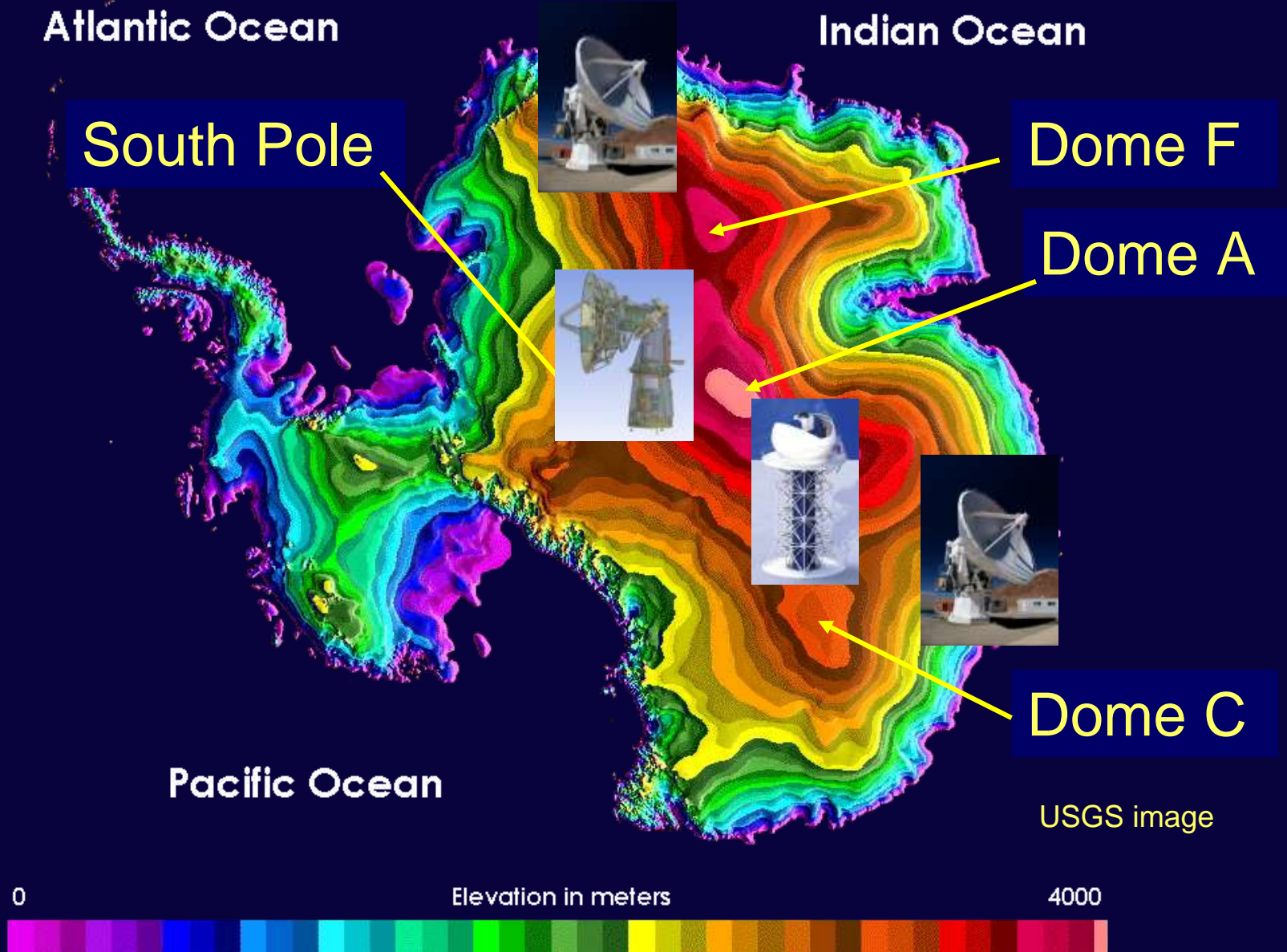
PCTJ designed with SISMA  
Shan et al. IRMMW-THz2018



# Experimental Setup Plan

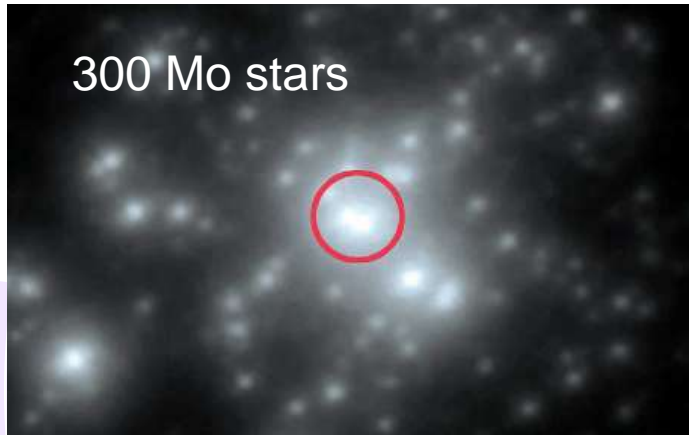


# Interferometry from Antarctica





# 30Dor region and R136



◆ [OIII] 88 $\mu$ m is observed widely distributed around R136

Contour: MIPS 24 $\mu$ m

Kawada et al. (2011)

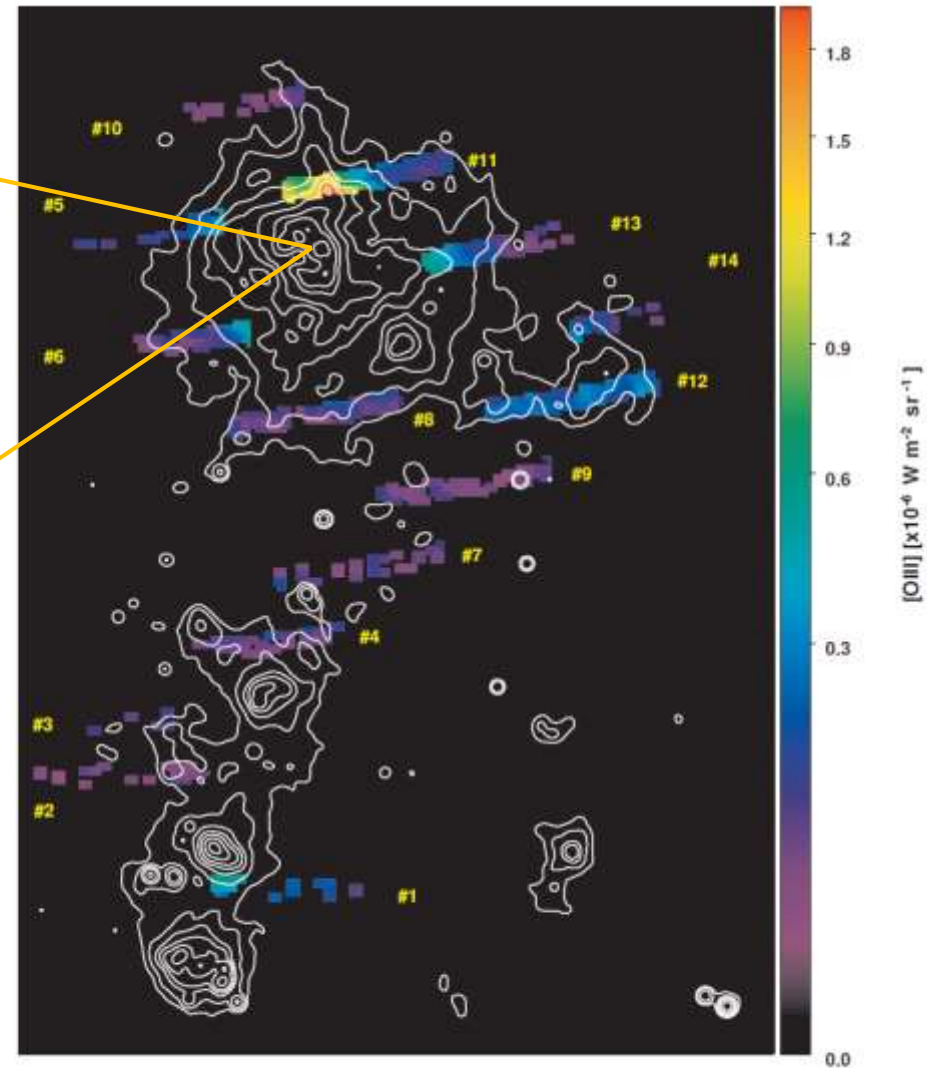
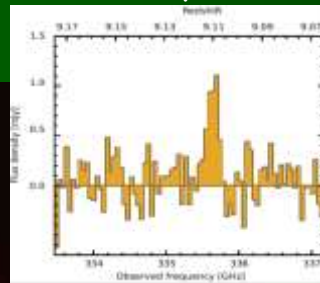


Fig. 3. [OIII] 88 $\mu$ m line intensity map, shown together with the MIPS 24 $\mu$ m contour map

# Heterodyne or Intensity ?

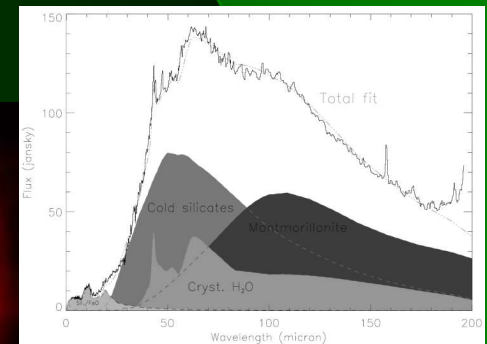
- Start with heterodyne interferometry
  - Shorter baselines, [NII]
- Challenge with intensity interferometry
  - Longer baselines, [OIII] and water ice feature

[OIII] 88 $\mu$ m



Hashimoto et al. (2018)

Water ice feature



HD142527

Malfait et al. (1999)

THz Observation

High Angular Resolution

THz Atmosphere

Intensity Interferometry